Bacterial Lipopolysaccharide Promotes Destabilization of Lung Surfactant-Like Films

Olga Cañadas,[†‡] Kevin M. W. Keough,[§] and Cristina Casals[†‡*]
[†]Departamento de Bioquímica y Biología Molecular I and [‡]CIBER Enfermedades Respiratorias, Universidad Complutense de Madrid, Madrid, Spain; and [§]Department of Biochemistry, Memorial University of Newfoundland, St. John's, Newfoundland, Canada

ABSTRACT The airspaces are lined with a dipalmitoylphosphatidylcholine (DPPC)-rich film called pulmonary surfactant, which is named for its ability to maintain normal respiratory mechanics by reducing surface tension at the air-liquid interface. Inhaled airborne particles containing bacterial lipopolysaccharide (LPS) may incorporate into the surfactant monolayer. In this study, we evaluated the effect of smooth LPS (S-LPS), containing the entire core oligosaccharide region and the O-antigen, on the biophysical properties of lung surfactant-like films composed of either DPPC or DPPC/palmitoyloleoylphosphatidylglycerol (POPG)/palmitic acid (PA) (28:9:5.6, w/w/w). Our results show that low amounts of S-LPS fluidized DPPC monolayers, as demonstrated by fluorescence microscopy and changes in the compressibility modulus. This promoted early collapse and prevented the attainment of high surface pressures. These destabilizing effects could not be relieved by repeated compression-expansion cycles. Similar effects were observed with surfactant-like films composed of DPPC/POPG/PA. On the other hand, the interaction of SP-A, a surfactant membrane-associated alveolar protein that also binds to LPS, with surfactant-like films containing S-LPS increased monolayer destabilization due to the extraction of lipid molecules from the monolayer, leading to the dissolution of monolayer material in the aqueous subphase. This suggests that SP-A may act as an LPS scavenger.

INTRODUCTION

The air-alveolar fluid interface is lined with a lipid-protein complex known as pulmonary surfactant. By reducing surface tension to low values, surfactant counteracts the tendency of the alveoli to collapse during expiration (1). In addition to its role in surface tension-related functions, pulmonary surfactant contains a number of host-defense molecules that are involved in the elimination of pathogens and pollutants. Surfactant protein A (SP-A) is a versatile recognition protein that binds to a great variety of immune and nonimmune ligands in the alveolar fluid and is principally involved in alveolar host defense (2,3). This protein is mainly associated with surfactant lipids (primarily dipalmitoylphosphatidylcholine (DPPC) (3,4), the major surfactant phospholipid) in the alveolar fluid. SP-A has also been shown to bind to other phospholipids and glycosphingolipids, as well as bacterial lipopolysaccharide (LPS) (4–8).

Bacterial LPS, or endotoxin, is a constituent of the cell wall of Gram-negative bacteria, which contribute to the local inflammation and systemic toxicity of Gram-negative infections. LPS consists of three different regions: lipid A, a core oligosaccharide region, and the O-polysaccharide specific chain, whose composition varies with the bacterial species involved (Fig. 1) (9). Lipid A contains the hydrophobic, membrane-anchoring region of LPS. Lipid A is the bioactive component that is responsible for some of the pathophysiology associated with severe Gram-negative bacterial infections in animals and humans. The core oligosaccharide region consists of a short, rather invariable chain of sugars that connects the lipid A anchor to the O-specific chain or O-antigen. The O-antigen is attached to the core oligosaccharide and extends from the core out into the environment. It consists of repeating oligosaccharide subunits made up of three to five sugars. The individual chains can vary in length, ranging up to 40 repeat units. The O-antigen is much longer than the core oligosaccharide and contains the hydrophilic domain of LPS. Wild-type enterobacterial species with O-chains are termed "smooth" and hence their LPS are called smooth LPS (S-LPS). Mutants that produce LPS lacking O-specific chains are termed "rough" (R) and their LPS are designated Ra, Rb, Rc, Rd, and Re in order of decreasing core length (9).

It is well known that chronic inhalation of organic dusts containing endotoxins produces a progressive decline in lung function (10). Most of the changes observed in acute lung injury induced by chronic inhalation of LPS may be dependent on LPS signaling through the functional Toll-like receptor-4 (TLR4) on alveolar and immune cells. LPS binding to TLR4 induces an inflammatory response and the recruitment of neutrophils into the air spaces (11). On the other hand, inhaled LPS molecules may incorporate into surfactant membranes, resulting in surfactant dysfunction (12), and surfactant dysfunction also contributes to significant morbidity and mortality with acute lung injury (1,13). Little is known about the effects of LPS on the biophysical properties of the surfactant monolayer. In this respect, we previously showed that Re-LPS, the minimal LPS form required for bacterial growth, interacts with DPPC films, and as a result, DPPC monolayers become more fluid and their surface tension properties are altered (8). In this study, we examined the effects of the whole

Submitted August 11, 2010, and accepted for publication November 9, 2010.

*Correspondence: ccasalsc@bio.ucm.es

Editor: Ka Yee C. Lee.

0006-3495/11/01/0108/9 $2.00

doi: 10.1016/j.bpj.2010.11.028

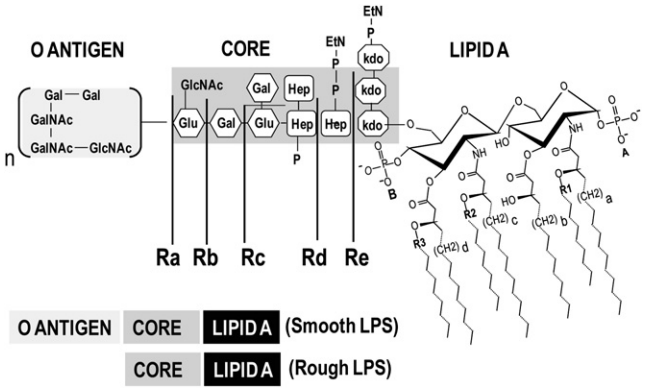

FIGURE 1 Chemical structure of bacterial LPS. LPS consists of three different regions: 1), a lipid component, termed lipid A, which contains the hydrophobic, membrane-anchoring region of LPS; 2), a core oligosaccharide section; and 3), an O-specific chain. Wild-type enterobacterial species with O-chains are termed "smooth" and hence their LPS are called smooth LPS (S-LPS). Mutants that produce LPS lacking O-specific chains are termed "rough" (R) and their LPS are designated as Ra, Rb, Rc, Rd, and Re in order of decreasing core length.

LPS molecule, containing the entire core oligosaccharide region and the O-antigen (S-LPS), on the physical properties of DPPC monolayers. We also tested the ability of S-LPS to interact with DPPC/palmitoyloleoylphosphatidylglycerol (POPG)/palmitic acid (PA) (28:9:5.6, w/w/w) membranes, which is a well-characterized lipid mixture that is often used in the formulation of new synthetic lung surfactants (14). In addition, given that SP-A is able to bind to the lipid A moiety of LPS (5,8), and this protein is associated with the surfactant monolayer (3,4,15,16), we investigated whether SP-A can minimize S-LPS effects on lung surfactant-like monolayers.

MATERIALS AND METHODS

Materials

DPPC, POPG, PA, and the fluorescent lipid probe NBD-PC were obtained from Avanti Polar Lipids (Birmingham, AL). S-LPS from *Escherichia coli* (serotype O55:B55) was purchased from Sigma (St. Louis, MO). The fluorescent probe used to chemically label SP-A, sulforhodamine 101 sulfonyl chloride or Texas Red (TR), was obtained from Molecular Probes (Eugene, OR). The organic solvents used to dissolve the lipids and S-LPS were high-performance liquid chromatography grade. The water used in all of the experiments and analytical procedures was deionized and doubly distilled in glass, with the second distillation being from dilute potassium permanganate solution.

Isolation and labeling of SP-A

SP-A was isolated from bronchoalveolar lavage of patients with alveolar proteinosis via sequential butanol and octylglucoside extraction (15–18). The purity of the SP-A was checked by one-dimensional sodium dodecyl sulfate polyacrylamide gel electrophoresis in 12% acrylamide under reducing conditions and mass spectrometry. The oligomerization state of the SP-A was assessed by electrophoresis under nondenaturing conditions, electron microscopy, and analytical ultracentrifugation as described elsewhere (17,18). The SP-A consisted of supratrimeric oligomers of at least 18 subunits. Each subunit had an apparent molecular mass of 36,000 Da. Fluorescently labeled SP-A with TR (TR-SP-A) was prepared as described previously (15,16).

Monolayer experiments

The monolayer experiments were performed with the use of a thermostated Langmuir-Blodgett trough (102 M microfilm balance; NIMA Technologies, Coventry, UK) equipped with an injection port and magnetic stirrer. The trough (total area = 100 cm^2) was equipped with two symmetrical movable barriers controlled by an electronic device. The subphase buffer employed was 5 mM Tris-HCl, 150 mM NaCl, 150 μM $CaCl_2$, pH 7.4 (buffer A).

Surface pressure-area isotherms

Monolayers of DPPC, S-LPS, DPPC/POPG/PA, or mixtures of DPPC and DPPC/POPG/PA with different amounts of S-LPS were formed by spreading 10 μL of a concentrated solution of the lipid dissolved in an organic solvent over the buffered saline subphase. Pure S-LPS was spread from a petroleum ether/chloroform/phenol 7:3:1 (v/v) solution. Pure DPPC, DPPC/POPG/PA, and mixtures of these lipids with S-LPS were spread from a solution of chloroform/methanol 3:1 (v/v) containing small amounts of petroleum ether/chloroform/phenol 7:3:1 (v/v). This solvent mixture did not affect the compression isotherms of either DPPC or DPPC/POPG/PA (data not shown). The organic solvent was allowed to evaporate for 10 min. The monolayer was then compressed at 50 cm^2/min while changes in surface pressure were monitored. The surface areas in the trough before and after compression were 76 and 22 cm^2, respectively. The data shown represent the average of seven measurements. All measurements were performed at 25°C. To evaluate the effect of human SP-A on π-A isotherms, the protein was injected into the subphase once the monolayer was formed, to yield a final protein concentration of 0.1 μg/mL. The surface pressure of the lipid monolayers before protein injection was 0.3 mN/m.

Cyclic compression-expansion isotherms

The hysteresis curves of the solvent-spread interfacial films were recorded by spreading the lipids with and without S-LPS at the air-water interface to a standard interfacial concentration of 90 $Å^2$/phospholipid molecule. Dynamic cycling commenced after a 15 min pause for solvent evaporation. Up to seven successive cycles of compression/expansion at the interface were recorded between maximum and minimum areas of 76 and 22 cm^2 (compression ratio 3.4:1) at a speed of 2 min per completed cycle. All measurements were performed at 25°C.

Relaxation kinetics

DPPC and DPPC/POPG/PA monolayers with and without S-LPS were compressed to a preset surface pressure kept constant by automatically adjusting the surface area of the trough through the movement of barriers. Once the desired surface pressure was reached, either SP-A or buffer was injected into the subphase. A relaxation curve was obtained by recording the trough surface area during the relaxation period (7).

Epifluorescence microscopy

Epifluorescence microscopy measurements were performed on a surface balance as described previously (7,8,15,16). DPPC, with and without S-LPS, was mixed with 1 mol % NBD-PC (based on the lipid content). Monolayers were formed by spreading the lipids onto a buffer A subphase. To evaluate the effect of SP-A on the morphology of DPPC/S-LPS films, TR-SP-A was injected into the subphase once the monolayers were formed, yielding a final protein concentration of 0.1 μg/mL. After a period of equilibration at 25 °C, the monolayer was compressed at a slow speed (20 mm^2/s or an initial rate of 0.13 $Å^2$/molecule/s). At selected surface pressures,

compression was halted, and a video recording was made over a 1 min period of both NBD-PC and TR fluorescence by switching fluorescence filter combinations. The video images were obtained with a CCD camera that records in black and white. Images were analyzed with digital image processing using JAVA 1.3 software (Jandel Scientific, San Rafael, CA) as discussed elsewhere (7,8,15,16).

RESULTS

Effect of S-LPS on DPPC monolayers

Fig. 2 *A* shows the surface pressure-area (π-A) isotherms for monolayers obtained by spreading either DPPC, S-LPS, or DPPC mixed with different amounts of S-LPS at 25 °C. Pure DPPC gave monolayers that exhibited a transition region between liquid expanded (LE) and tightly packed tilted condensed (TC) phases at surface pressures in the range of 7–12 mN/m on a buffer A subphase (Fig. 2 *A*, *solid line*, and Fig. 3). The collapse pressure for this phospholipid was close to 70 mN/m. The inset of Fig. 2 *A* shows that S-LPS did not form stable monolayers when deposited at

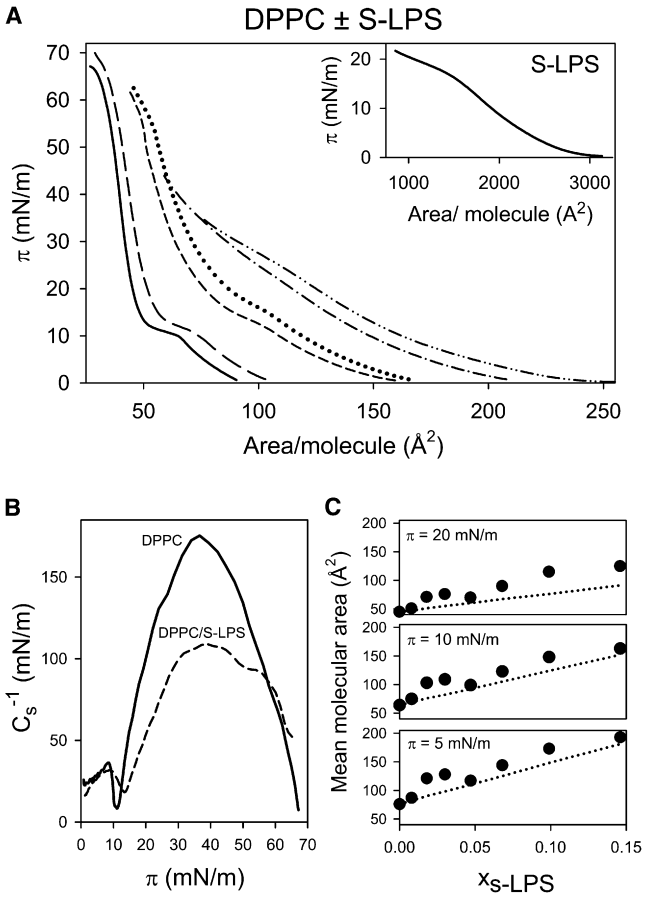

FIGURE 2 (*A*) Surface pressure (π)-area isotherms of DPPC/S-LPS mixed monolayers as a function of S-LPS molar fraction, $X_{S\text{-}LPS}$: 0.0 (——); 0.01 (— —); 0.03 (——); 0.07 (- - - - -); 0.1 (— · —); and 0.15 (— ·· —). The monolayers were compressed at 50 cm^2/min on a subphase containing buffer A. The temperature of the subphase was 25.0 ± 0.1°C. (*B*) Compressibility modulus (C_s^{-1})-surface pressure dependencies for DPPC monolayers in the absence (——) and presence (- - - - -) of $X_{S\text{-}LPS} = 0.02$. (*C*) Mean molecular area of DPPC/S-LPS mixed monolayers as a function of $X_{S\text{-}LPS}$ at three surface pressures. The dotted lines are the theoretical variations assuming the additivity rule. Error bars are within the size of the symbol. Data shown in *A*–*C* are the means of seven independent measurements.

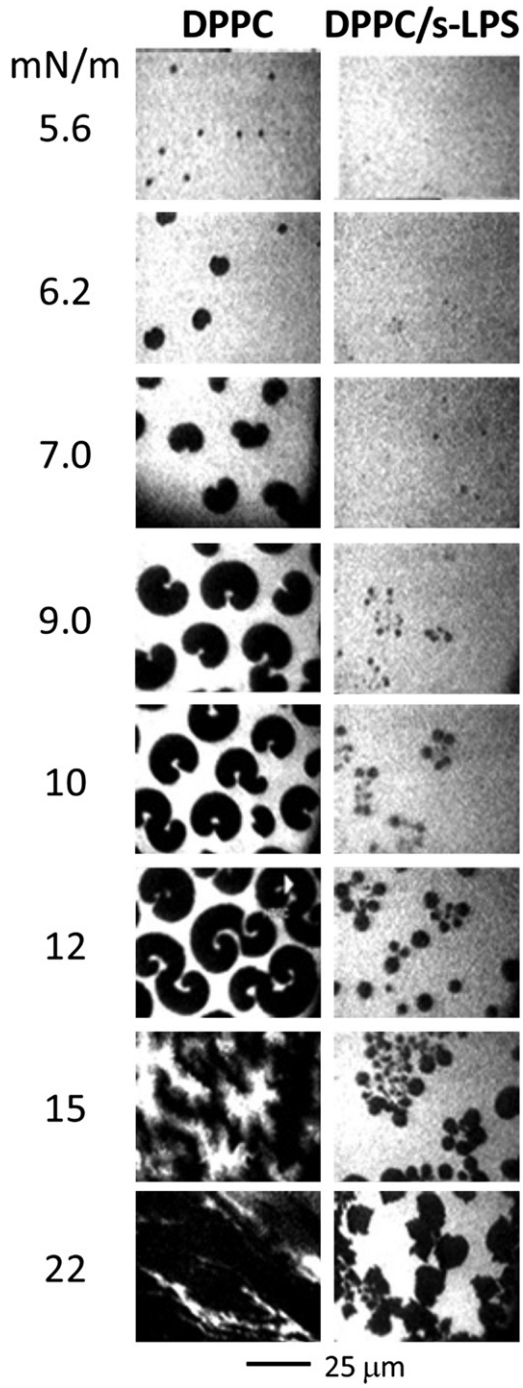

FIGURE 3 Typical fluorescence images obtained from pure DPPC and DPPC/S-LPS ($X_{S\text{-}LPS} = 0.02$) mixed monolayers containing 1 mol % NBD-PC at the indicated surface pressures. The monolayers were spread on a subphase containing buffer A. The bright background indicates the phase containing the fluorescent probe NBD-PC. The scale bar is 25 μm.

the air-water interface. Cospread DPPC/S-LPS monolayers exhibited a behavior intermediate between those displayed by single components (Fig. 2 *A*, *broken lines*). The presence of S-LPS concentrations as low as $X_{S\text{-}LPS} = 0.01$ increased the surface pressure at which the LE/TC phase transition occurred, which indicates that S-LPS stabilizes the LE phase. As the amount of S-LPS increased, the LE/TC phase coexistence plateau observed for pure DPPC gradually disappeared and the curves were progressively shifted toward higher values of mean molecular area. S-LPS promoted early collapse of DPPC films even at concentrations as low as $X_{S\text{-}LPS} = 0.03$, which indicates an S-LPS-induced destabilization of the monolayers at higher surface pressures.

Compression isotherms were analyzed in terms of the reciprocal isothermal compressibility (C_s^{-1}, the compressibility modulus) defined as:

$$C_s^{-1} = -A\left(\frac{d\pi}{dA}\right)_T, \qquad (1)$$

where A is the molecular area. Representative C_s^{-1} versus π curves recorded at $X_{S\text{-}LPS}$ of either 0 or 0.02 are illustrated in Fig. 2 *B*. In pure DPPC films, the LE/TC phase transition appeared as a pronounced minimum at a surface pressure of ~11 mN/m that separated LE ($C_s^{-1} = 12.5$–50 mN/m) and TC ($C_s^{-1} = 100$–200 mN/m) phases. The incorporation of S-LPS molecules into DPPC monolayers resulted in a shift of the discontinuity between LE and TC phases to higher surface pressures (Fig. 2 *B*). This indicates that S-LPS would induce the stabilization of the LE phase, i.e., a fluidizing effect on the film would occur. The values for the maximum in compressibility modulus ($C_s^{-1}{}_{max}$) decreased in proportion to the increase of $X_{S\text{-}LPS}$ (Table 1). At $X_{S\text{-}LPS} = 0.10$, the $C_s^{-1}{}_{max}$ diminished to values typical of the pure LE monolayer (47 mN/m; Table 1), which suggests that cospread S-LPS renders the DPPC monolayer fluid.

To investigate the thermodynamic stability of mixed lipid/S-LPS monolayers compared with the monolayers of the pure component, we evaluated the excess Gibbs free energy of mixing, ΔG_{ex}, by integrating the surface pressure-area isotherm up to the selected surface pressure π (19):

$$\Delta G_{ex} = \int_0^{\pi} (A_{12} - [x_1A_1 + x_2A_2])d\pi, \qquad (2)$$

where x_1 and x_2 are the molar fractions of the lipids and S-LPS, respectively, and A_1 and A_2 are the molecular areas occupied by the lipids and S-LPS, respectively. A_{12} is the molar area occupied by mixed lipid/S-LPS films. Positive ΔG_{ex} values indicate thermodynamic instability of the mixed monolayers, whereas negative ΔG_{ex} values suggest thermodynamic stability of the film. In the case of ideal mixing between monolayer components, ΔG_{ex} attains a zero value (19).

Table 1 shows that at very low S-LPS concentrations ($X_{S\text{-}LPS} \leq 0.03$), ΔG_{ex} is negative, suggesting stable films. This trend disappears progressively with increasing S-LPS concentration. For $X_{S\text{-}LPS} \geq 0.05$, ΔG_{ex} values are positive, indicating the destabilization of the monolayers in agreement with the S-LPS-promoted early collapse of DPPC films described above. To further characterize the interactions between both molecules, the mean area per molecule was plotted as a function of the mole fraction of S-LPS at three surface pressures: 5, 10, and 20 mN/m (Fig. 2 *C*). The results show that, for all surface pressures studied, positive deviations from ideal behavior (represented by the *dotted lines*) were observed, indicating repulsive interactions between DPPC and S-LPS. For these studies, the molecular area of S-LPS was experimentally determined from isotherms assuming a molecular weight for S-LPS of 10,000. For high surface pressures, experimental values of S-LPS molecular area cannot be determined due to the low surface activity of S-LPS (Fig. 2 *A*, *inset*).

To determine whether S-LPS is excluded from mixed DPPC/S-LPS films upon compression, we examined the effect of S-LPS on the compressibility modulus of cycled DPPC monolayers at a standard interfacial concentration of 90 Å^2/phospholipid molecule. In pure DPPC films, C_s^{-1} remained relatively unchanged during the seven repeated compressions (Table 2). Remarkably, in DPPC/S-LPS films ($X_{S\text{-}LPS} = 0.02$), C_s^{-1} increased from the first to the fourth compression and remained relatively unchanged during the next three compressions (Table 2). This indicates a gradual refining of the films by squeezing out S-LPS molecules from the interface. However, the compressibility modulus did not approach that of pure DPPC monolayers at any given surface pressure, indicating that S-LPS molecules were not completely removed from the monolayer by repeated compression-expansion cycles.

To characterize the effects of S-LPS on lipid lateral organization of DPPC films, epifluorescence microscopy images of mixed DPPC/S-LPS monolayers were recorded. Fig. 3 compares two sets of images: 1), typical fluorescence images obtained from DPPC/S-LPS ($X_{S\text{-}LPS} = 0.02$) monolayers

TABLE 1 Effect of S-LPS on the compressibility modulus, $C_s^{-1}{}_{max}$, and excess Gibbs free energy of mixing, ΔG_{ex}, of DPPC and DPPC/POPG/PA monolayers

	DPPC		DPPC/POPG/PA	
$X_{S\text{-}LPS}$	$C_s^{-1}{}_{max}$ (mN/m)	ΔG_{ex} (kJ/mol)	$C_s^{-1}{}_{max}$ (mN/m)	ΔG_{ex} (kJ/mol)
0.00	175 ± 2	0	98 ± 2	0
0.01	148 ± 4	−0.16 ± 0.04	82 ± 2	0.16 ± 0.04
0.02	109 ± 1	−0.14 ± 0.03	73 ± 1	0.19 ± 0.03
0.03	120 ± 2	−0.06 ± 0.02	81 ± 1	0.40 ± 0.02
0.05	84 ± 2	0.71 ± 0.05	67 ± 1	0.60 ± 0.05
0.07	104 ± 1	0.46 ± 0.04	59 ± 1	1.69 ± 0.04
0.10	47 ± 3	0.90 ± 0.03	47 ± 1	1.42 ± 0.03
0.15	41 ± 2	2.19 ± 0.05	32 ± 1	nd
1.00	29 ± 1	0	29 ± 1	0

The upper limit of surface pressure used in the calculation of ΔG_{ex} according to Eq. 2 was 20 mN/m. Results represent the mean ± SD determined from six independent experiments.

TABLE 2 Effect of S-LPS ($x_{s\text{-}LPS} = 0.02$) on the compressibility modulus of cycled DPPC and DPPC/POPG/PA films with the number of compressions, at 20, 30, and 40 mN/m

		C_s^{-1} (mN/m)		
Monolayer	Cycle	20 mN/m	30 mN/m	40 mN/m
DPPC	1	100 ± 2	157 ± 3	170 ± 2
	2–7	101 ± 1	157 ± 2	173 ± 2
DPPC/s-LPS	1	59 ± 1	95 ± 2	105 ± 1
	2	59 ± 1	118 ± 2	120 ± 1
	3	60 ± 1	128 ± 1	127 ± 1
	4–7	63 ± 1	134 ± 1	129 ± 1
DPPC/POPG/PA	1	68 ± 1	98 ± 1	84 ± 1
	2–7	66 ± 1	95 ± 1	82 ± 1
DPPC/POPG/PA/S-LPS	1	62 ± 2	73 ± 1	59 ± 1
	2–7	62 ± 2	76 ± 2	62 ± 2

Measurements were performed at a standard interfacial concentration of 90 Å^2/phospholipid molecule.

containing 1 mol % NBD-PC at the indicated surface pressures; and 2), recently reported epifluorescence images of pure DPPC monolayers spread on the same buffered saline subphase (8). The fluorescent dye (NBD-PC) selectively dissolved in the LE phase, which appeared bright in the fluorescence images of the monolayers (8,15,16). The appearance of nonfluorescent solid domains coincided with the onset of the LE/TC transition. In DPPC monolayers, the fluorescence of NBD-PC showed kidney-shaped dark solid domains typical of the LE/TC coexistence region of DPPC monolayers over the range of 7–12 mN/m. At higher surface pressures, nonfluorescent solid domains grew to occupy most of the monolayer (Fig. 3). The presence of low amounts of S-LPS ($X_{S\text{-}LPS} = 0.02$) in mixed DPPC/S-LPS monolayers increased the surface pressure where dark, probe-excluded domains appear. This indicates that S-LPS increases the transition pressure from the disordered to the more-ordered phase in which the fluorescent lipid does not incorporate, in accordance with the S-LPS-promoted displacement of the LE/TC phase transition of DPPC isotherms described above. S-LPS also altered the morphology of the DPPC-rich dark domains, which changed from kidney shapes to multisized circular domains shaped like bunches of grapes. In addition, the ordered dark domains decreased in size and area coverage (Fig. 3). This indicates that S-LPS induced the fluidification of the DPPC monolayer, in agreement with the S-LPS-promoted decrease in the compressibility modulus of DPPC films (Fig. 2 *B* and Table 1).

Effect of S-LPS on DPPC/POPG/PA monolayers

We also tested the effect of S-LPS on a DPPC/POPG/PA mixture (28:9:5.6, w/w/w), a surfactant-like lipid composition that is frequently used in the formulation of new synthetic lung surfactants (14). As was observed for the DPPC/S-LPS films, S-LPS destabilized the DPPC/POPG/PA monolayers, decreasing the collapse pressure of these films (Fig. 4 *A*). This is consistent with the positive values

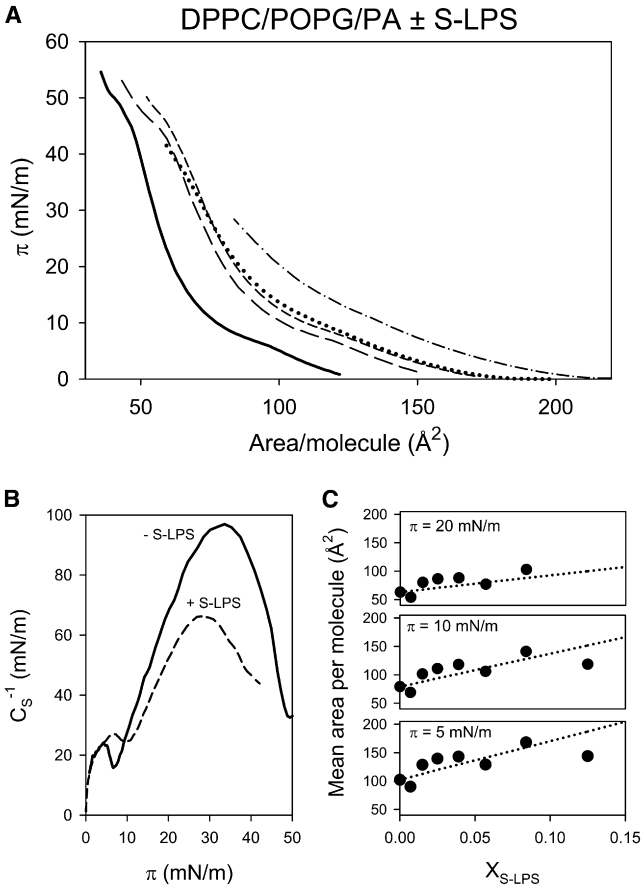

FIGURE 4 (*A*) Surface pressure (π)-area isotherms of DPPC/POPG/PA/S-LPS mixed monolayers as a function of S-LPS molar fraction, $X_{S\text{-}LPS}$: 0.0 (——); 0.01 (— —); 0.02 (- - - -); 0.04 (●●●●●●); and 0.08 (— · —). The monolayers were compressed at 50 cm2/min on a subphase containing buffer A. The temperature of the subphase was 25.0 ± 0.1°C. (*B*) Compressibility modulus (C_s^{-1})-surface pressure dependencies for DPPC/POPG/PA monolayers in the absence (—) and presence (- - - - -) of $X_{S\text{-}LPS} = 0.04$. (*C*) Mean molecular area of DPPC/POPG/PA/S-LPS mixed monolayers as a function of $X_{S\text{-}LPS}$ at three surface pressures. The dotted lines are the theoretical variations assuming the additivity rule. Error bars are within the size of the symbol. Data shown in *A–C* are the means of seven independent measurements.

of ΔG_{ex} obtained for $X_{S\text{-}LPS} \geq 0.01$ (Table 1). In addition, S-LPS fluidized DPPC/POPG/PA films, as determined by the decrease in $C_s^{-1}{}_{max}$ (Table 1 and Fig. 4 *B*). Although S-LPS exerted a similar effect on pure DPPC and DPPC/POPG/PA membranes, the compressibility modulus of mixed DPPC/POPG/PA/S-LPS ($X_{s\text{-}LPS} = 0.02$) films remained unchanged upon cycling (Table 2), which suggests that S-LPS was not excluded from the interfacial film upon compression.

SP-A interaction with surfactant-like films containing S-LPS

To characterize the interaction between SP-A and surfactant-like films containing S-LPS, we measured the π-A

isotherms of DPPC and DPPC/POPG/PA films, with and without S-LPS ($X_{S\text{-}LPS} = 0.02$), before and after SP-A adsorption at the air-water interface. Fig. 5 shows that SP-A caused an expansion of the DPPC, DPPC/S-LPS, DPPC/POPG/PA, or DPPC/POPG/PA/S-LPS isotherms. SP-A also expanded pure S-LPS films (see Fig. S1 in the Supporting Material). Given that SP-A alone did not detectably adsorb to the interface at the concentration used in these experiments (0.1 μg/mL SP-A), these results indicate that the protein interacted with these lipid monolayers enough to perturb the usual lipid packing. The perturbing influence of SP-A on DPPC and DPPC/POPG/PA monolayers was observed up to ~30 and 49 mN/m, respectively. Above these surface pressures, the mean area per lipid molecule in the DPPC and DPPC/POPG/PA films was the same in the absence and presence of SP-A in the subphase, suggesting that the protein was excluded from the monolayers (8,15). The stronger effect of SP-A on DPPC/POPG/PA monolayers may be due to the greater fluidity of these films (Table 1), which would favor the retention of the protein in the monolayer upon film compression.

On the other hand, the perturbing influence of SP-A on DPPC/S-LPS and DPPC/POPG/PA/S-LPS films was observed above 34 and 30 mN/m, respectively. Beyond these surface pressures, the isotherms of DPPC/S-LPS and DPPC/POPG/PA/S-LPS in the presence of SP-A were displaced toward molecular areas smaller than the corresponding isotherms in the absence of SP-A. These results may indicate that the exclusion of the protein from these monolayers is accompanied by the extraction of some lipid molecules. This hypothesis is reinforced by the fact that both DPPC/S-LPS and DPPC/POPG/PA/S-LPS isotherms reached a maximum surface pressure that was lower in the presence of SP-A than in its absence (Fig. 5). This would indicate that the exclusion of SP-A along with other components of the interfacial film renders the monolayers unstable.

To demonstrate that SP-A is able to extract lipids from DPPC/S-LPS and DPPC/POPG/PA/S-LPS films but not from DPPC and DPPC/POPG/PA films, we measured the relaxation time of the surface area of these films after compression to 20 mN/m, in the absence and presence of 0.1 μg/mL SP-A (Fig. 6, *A* and *B*). The presence of SP-A in the subphase significantly increased the relaxation rate of DPPC and DPPC/POPG/PA films containing S-LPS, but not of those without S-LPS. As a result, the area loss at a given time was greater in the presence of SP-A than in its absence. Similar results were found with films compressed to 30 mN/m (data not shown). These results suggest that the SP-A-induced molecular loss of surfactant-like monolayers containing S-LPS may depend on the specific interaction of SP-A with S-LPS. To determine whether the SP-A-induced molecular loss of monolayers containing S-LPS was due to the dissolution of lipid molecules into the subphase through diffusion (desorption) or to the transformation of the two-dimensional monolayer material into three-dimensional aggregates, the relaxation curves were analyzed according to the model proposed by Smith and Berg (20). Fig. 6, *C* and *D*, show the variance of $-\log(A/A_0)$ with $\sqrt{t}$ for DPPC and DPPC/POPG/PA films, with and without S-LPS, in the absence and presence of SP-A, where A and A_0 are the trough surface areas at a given time t and at $t = 0$, respectively. Thus, if the monolayer molecular loss were due to dissolution of lipid molecules into the subphase, a linear relationship between $-\log(A/A_0)$ and the square root of time, $\sqrt{t}$, would be obtained (20). The nearly linear relationship of the data confirms a loss of monolayer material from the interface due to partial desorption of film molecules into the aqueous subphase. Data for S-LPS containing DPPC/POPG/PA films in the presence of SP-A (Fig. 6 *D*) indicate that the desorption mechanism consists of two dissolution steps of different constant rates, as previously described in other systems (21). On the other hand, deviations from linearity when $\sqrt{t}$ is small for data of DPPC/S-LPS films in the presence of SP-A (Fig. 6 *C*) may be due to rearrangement effects as described previously (20).

Finally, we performed epifluorescence measurements to examine the effect of SP-A binding to DPPC/S-LPS ($X_{S\text{-}LPS} = 0.02$) monolayers on the morphology of these films. Fig. 7 shows that the DPPC/S-LPS films displayed profound changes upon incorporation of the protein. Our results indicate that for DPPC/S-LPS/SP-A monolayers, microheterogeneous surface phases coexist over the range

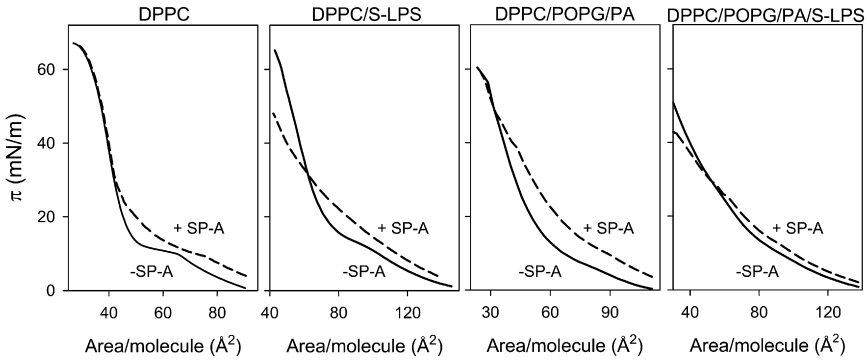

FIGURE 5 SP-A effect on the pressure-area isotherms of DPPC, DPPC/S-LPS ($X_{S\text{-}LPS} = 0.02$), DPPC/POPG/PA, and DPPC/POPG/PA/S-LPS ($X_{S\text{-}LPS} = 0.02$) monolayers spread onto a subphase containing buffer A. The protein was injected into the subphase once the monolayers were formed to yield a final protein concentration of 0.1 μg/mL SP-A. The surface pressure of the lipid monolayers before injection of the protein was 0.3 mN/m. The temperature of the subphase was 25.0 ± 0.1 °C. Data shown are the means of seven independent measurements.

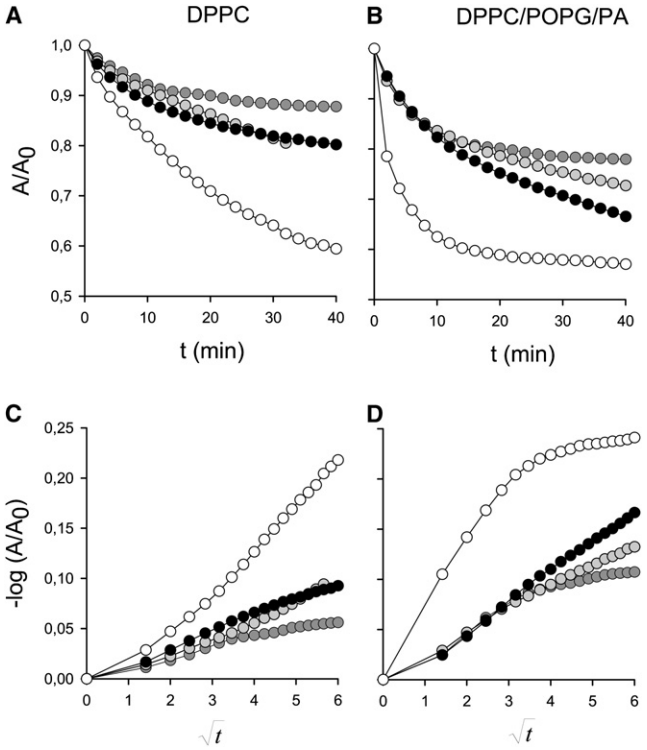

FIGURE 6 Relaxation kinetics of (*A*) DPPC and DPPC/S-LPS ($X_{S\text{-}LPS} = 0.02$) films and (*B*) DPPC/POPG/PA and DPPC/POPG/PA/S-LPS ($X_{S\text{-}LPS} = 0.02$) monolayers in the absence and presence of SP-A (0.1 μg/mL), compressed to a surface pressure of 20 mN/m. A and A_0 are the trough surface areas at a given time t and $t = 0$, respectively. The temperature of the subphase was 25.0 ± 0.1 °C. Constant pressure relaxation data of (*C*) DPPC and DPPC/S-LPS films and (*D*) DPPC/POPG/PA and DPPC/POPG/PA/S-LPS monolayers in the absence and presence of 0.1 μg/mL SP-A at a surface pressure of 20 mN/m expressed as $-\log(A/A_0)$ versus $\sqrt{t}$, to determine whether monolayer desorption is due to dissolution of lipid molecules into the subphase or to monolayer transformation into three-dimensional aggregates. Data shown are the means of seven independent measurements. The standard deviation for each relaxation kinetic was too small to be displayed by error bars. Symbols: pure lipid monolayers, dark gray circles; mixed lipid/S-LPS monolayers, solid circles; pure lipid monolayers plus SP-A, light gray circles; mixed lipid/S-LPS monolayers plus SP-A, white circles.

of surface pressures studied (7–30 mN/m). It is unlikely that the dark and fluid domains in DPPC/S-LPS/SP-A monolayers correspond to solid and fluid phases, respectively. In this respect, we found that at $\pi \geq 9.5$ mN/m, the fluorescence of the protein (TR-SP-A) is distributed in both dark and brilliant domains. The dark domains became fuzzy and penetrated by fluorescent points, indicating that TR-SP-A incorporated in these dark regions. Given that SP-A interacts with both kinds of lipids of these mixed films (i.e., DPPC (Fig. 5) and S-LPS (Fig. S1)), SP-A may reduce interactions between the pure component molecules themselves upon compression. As a result, at $\pi = 30$ mN/m, the dark domains were smaller in size and their physical state was likely different in DPPC/S-LPS/SP-A mixed monolayers than in the dark domains of the DPPC/S-LPS monolayers.

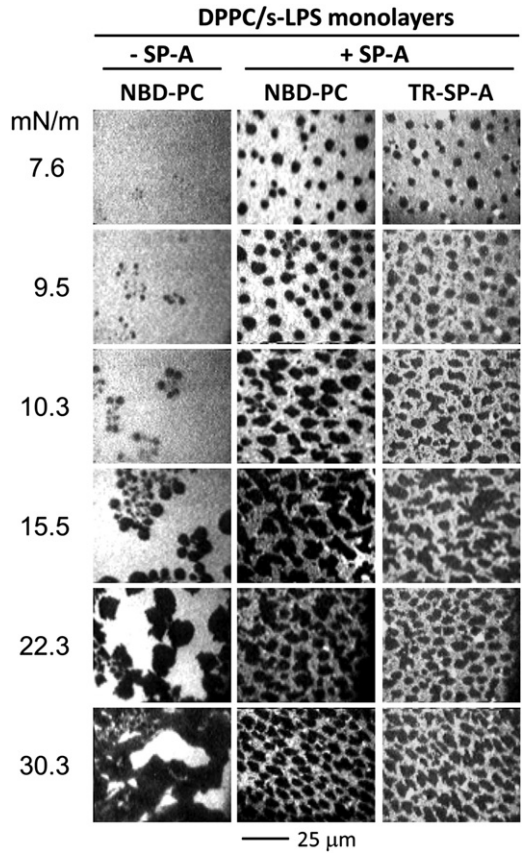

FIGURE 7 SP-A effect on the morphology of DPPC/S-LPS ($X_{S\text{-}LPS} = 0.02$) mixed monolayers containing 1 mol % NBD-PC spread onto a subphase containing buffer A. TR-SP-A was injected into the subphase once the monolayer was formed to yield a final protein concentration of 0.1 μg/mL TR-SP-A. The surface pressure of the lipid monolayers before injection of the protein was 0.3 mN/m. Images were recorded at the surface pressures indicated through filters selecting fluorescence from either NBD-PC (emission centered at 520 nm) or TR-SP-A (emission centered at 590 nm). The scale bar is 25 μm.

DISCUSSION

Upon inhalation of airborne particles containing endotoxins, LPS molecules would arrive at the lung alveolar surface from the air side of the monolayer. Therefore, LPS would interact with a high hydrophobic surface of lipid chains. Little is known about the direct effects of LPS on the biophysical properties of the lung surfactant-like lipid monolayers. In this study our main objective was to characterize the effect of the whole LPS molecule, containing the entire core oligosaccharide region and the O-antigen (S-LPS) (Fig. 1), on the physical properties of DPPC and DPPC/POPG/PA (28:9:5.6, w/w/w) monolayers. In addition, we investigated whether SP-A, which is an LPS-binding protein in the alveolar fluid, could modify S-LPS effects on surfactant-like films.

Our results demonstrate that mixed DPPC/S-LPS films (Fig. 2 *A*) showed nonideal mixing behavior (Fig. 2 *C*) and film instability at $X_{S\text{-}LPS} \geq 0.05$ ($\Delta G_{ex} > 0$; Table 1).

The repulsive interactions between these lipids decreased the overall packing density of the DPPC/S-LPS mixture, favoring the LE phase over the more rigid TC phase. This was reflected in 1), the S-LPS-induced shift of the LE/TC phase transition of DPPC monolayers to higher surface pressures (Figs. 2 *B* and 3); 2), the S-LPS-induced decrease of ${C_s}^{-1}{}_{\max}$ values, which at $X_{S\text{-}LPS} \geq 0.1$ changed from values typical of the TC phase of pure DPPC films to values typical of the LE phase (Table 1); and 3), the splitting of DPPC-rich TC domains into smaller ones and the reduction in the number of these domains as observed by fluorescence microscopy (Fig. 3). The presence of S-LPS molecules in DPPC films promoted earlier collapse and thus prevented the attainment of high surface pressures (Fig. 2 *A*). Several parts of the S-LPS molecule could contribute to the S-LPS fluidizing effect on DPPC monolayers. The lipid A and core regions of S-LPS might act as a spacer between DPPC molecules, as previously reported for Re-LPS (8). In addition, the O-antigen is flexible enough to be stretched out to significant distances and to cross over with other O-chains. Thus, there might be an increased interaction between neighboring S-LPS molecules through the O chain (and possibly the outer core region) (22). This type of interaction between neighboring S-LPS molecules would explain why the insertion of S-LPS into DPPC monolayers resulted in film instability at $X_{S\text{-}LPS} \geq 0.05$ ($\Delta G_{ex} > 0$), indicating that mutual interactions between DPPC and S-LPS are weaker than the interactions between the pure component molecules themselves.

We also explored the interaction of S-LPS with films of the lipid mixture DPPC/POPG/PA, which is often used in the formulation of new synthetic lung surfactants (15). Our results show that S-LPS also exerted a destabilizing and fluidizing effect on DPPC/POPG/PA monolayers (Fig. 4 and Table 1). However, there were some differences between the S-LPS interactions with DPPC and DPPC/POPG/PA monolayers. In the DPPC/S-LPS films, the interactions were repulsive, whereas a more complex behavior was observed between DPPC/POPG/PA and S-LPS, with repulsive and attractive interactions that could be due to selective interactions of S-LPS with the bacterial membrane lipid POPG. The different interaction of S-LPS with DPPC and DPPC/POPG/PA monolayers would explain the removal of part of the S-LPS molecules from DPPC/S-LPS films upon compression and the retention of S-LPS in DPPC/POPG/PA/S-LPS monolayers.

The alveolar fluid contains several proteins and peptides that are able to bind to LPS (e.g., α-defensin, cathelicidin, lactoferrin, CD14, LBP, and surfactant collectins). SP-A is one of these LPS-binding proteins, with the peculiarity that this protein is associated with the surfactant monolayer. Thus, SP-A is in the initial defense barrier against inhaled airborne particles, toxins, and pathogens. Given that SP-A binds to the lipid A moiety of LPS (5,8), its interaction with Re-LPS is favored over S-LPS. There is no agreement on whether SP-A binds directly to S-LPS. For instance, a study using hydrophobic microtiter plates showed that SP-A does not bind to S-LPS (23), whereas results obtained with hydrophilic microtiter plates indicated that SP-A binds to S-LPS molecules (24). This discrepancy may be explained by considering that when the lipid A of S-LPS is accessible to SP-A, i.e., in hydrophilic microtiter plates or monolayers in the LE phase (Fig. 5), SP-A is capable of binding to it. In contrast, however, when the bulky headgroup of S-LPS hinders the access of SP-A to the lipid A (i.e., in hydrophobic microtiter plates), no binding is observed. Our results show that SP-A binds to S-LPS molecules in both pure S-LPS films (Fig. S1) and surfactant-like films containing S-LPS (Figs. 5 and 6). It is likely that the low lipid packing density in both pure S-LPS and surfactant-like films containing S-LPS at low surface pressure allows binding of SP-A to S-LPS.

SP-A binding to DPPC/S-LPS films resulted in profound changes in the physical properties and morphology of these monolayers. DPPC/S-LPS/SP-A isotherms did not show a two-dimensional surface pressure-induced phase transition (Fig. 5). Likewise, epifluorescence microscopy of DPPC/S-LPS mixed monolayers ($X_{S\text{-}LPS} = 0.02$) containing 1 mol % NBD-PC revealed that SP-A induced the phase coexistence of microheterogeneous dark and bright domains over the range of surface pressures studied (7–30 mN/m) (Fig. 7). It is possible that the lack of defined surface pressure-induced phase transitions in DPPC/S-LPS/SP-A compression isotherms is due to the complexity of interactions between the components of this multicomponent mixture. This hypothesis is reinforced by the fact that fluorescent TR-SP-A partitions in both dark (ordered) and bright (disordered) lipid domains (Fig. 7), which suggests that SP-A may rearrange the lipids to form some kind of self-assembled structure that combines both the lipid and the protein. This would reduce interactions between pure S-LPS molecules themselves (or pure DPPC) upon compression, and might decrease the immiscibility of DPPC and S-LPS.

Of interest, the compression isotherms of DPPC/S-LPS and DPPC/POPG/PA/S-LPS monolayers plus SP-A indicate a destabilizing effect of the protein on these monolayers, and suggest that SP-A may facilitate the extraction of lipid molecules from these films. The relaxation kinetics at constant surface pressure of DPPC and DPPC/POPG/PA monolayers with and without S-LPS (Fig. 6) demonstrated that SP-A extracts lipid molecules from monolayers containing S-LPS. Thus, SP-A-induced molecular loss of monolayers seems to depend on the specific interaction of SP-A with S-LPS, and results from the dissolution of lipid molecules into the subphase through diffusion. This effect was stronger on DPPC/POPG/PA/S-LPS than on DPPC/S-LPS films, probably due to the greater fluidity of the former monolayer (Table 2), which would facilitate the interaction of SP-A with the lipid A moiety of S-LPS.

SP-A-induced desorption of S-LPS molecules would be favored by the aqueous solubility of S-LPS, and is consistent with a scavenger role for the protein. This extraction seemed to be accompanied by the withdrawal of some lipid molecules from the monolayer, since the collapse pressure for DPPC/S-LPS and DPPC/POPG/PA/S-LPS monolayers was lower in the presence of SP-A than in its absence. Under physiological conditions, removal of some DPPC molecules from the monolayer could be compensated for by fresh surfactant material continuously incorporating into the monolayer. The extraction of S-LPS mediated by SP-A from the monolayer would facilitate S-LPS clearance by alveolar macrophages. In addition, SP-A is able to decrease the macrophage proinflammatory response to S-LPS, limiting excessive inflammation in the alveolar fluid that would compromise gas exchange (2,3,23,24).

In summary, the interaction of S-LPS with DPPC and DPPC/POPG/PA monolayers significantly fluidized these films, promoting early collapse and preventing the achievement of high surface pressures. S-LPS may exert these fluidizing effects by acting as a spacer between the lipid molecules and interfering with lipid packing upon compression. SP-A, with its ability to bind to both S-LPS and DPPC, causes pronounced alterations in both DPPC/S-LPS and DPPC/POPG/PA/S-LPS films, promoting the formation of more fluid and unstable monolayers by favoring the dissolution of the film material containing S-LPS into the subphase.

SUPPORTING MATERIAL

A figure is available at http://www.biophysj.org/biophysj/supplemental/S0006-3495(10)01426-8.

We thank I. García-Verdugo for his help on this article.

This work was supported by the Ministerio de Ciencia e Innovación (SAF2009-07810), Instituto de Salud Carlos III (CIBERES-CB06/06/0002), CAM (S-BIO-0260-2006), Fundación Médica MM, and the Canadian Institutes of Health Research (CIHR MT-9361 to K.M.W.K.).

REFERENCES

1. Zuo, Y. Y., R. A. Veldhuizen, …, F. Possmayer. 2008. Current perspectives in pulmonary surfactant—inhibition, enhancement and evaluation. *Biochim. Biophys. Acta.* 1778:1947–1977.
2. Wright, J. R. 2005. Immunoregulatory functions of surfactant proteins. *Nat. Rev. Immunol.* 5:58–68.
3. Casals, C., and I. García-Verdugo. 2005. Molecular and functional properties of surfactant protein A. *In* Lung Surfactant Function and Disorder. K. Nag, editor. Taylor & Francis Group, Boca Raton, FL. 59–86.
4. Casals, C. 2001. Role of surfactant protein A (SP-A)/lipid interactions for SP-A functions in the lung. *Pediatr. Pathol. Mol. Med.* 20:249–268.
5. Van Iwaarden, J. F., J. C. Pikaar, …, J. A. van Strijp. 1994. Binding of surfactant protein A to the lipid A moiety of bacterial lipopolysaccharides. *Biochem. J.* 303:407–411.
6. García-Verdugo, I., F. Sánchez-Barbero, …, C. Casals. 2005. Interaction of SP-A (surfactant protein A) with bacterial rough lipopolysaccharide (Re-LPS), and effects of SP-A on the binding of Re-LPS to CD14 and LPS-binding protein. *Biochem. J.* 391:115–124.
7. Cañadas, O., I. García-Verdugo, …, C. Casals. 2008. SP-A permeabilizes lipopolysaccharide membranes by forming protein aggregates that extract lipids from the membrane. *Biophys. J.* 95:3287–3294.
8. García-Verdugo, I., O. Cañadas, …, C. Casals. 2007. Surfactant protein A forms extensive lattice-like structures on 1,2-dipalmitoylphosphatidylcholine/rough-lipopolysaccharide-mixed monolayers. *Biophys. J.* 93:3529–3540.
9. Seydel, U., A. B. Schormm, …, K. Brandenburg. 2000. Chemical structure, molecular conformation and bioreactivity of endotoxins. *In* Chemical Immunology: CD14 in the Inflammatory Response. R. S. Jack, editor. Karger, Basel. 5–24.
10. Deetz, D. C., P. J. Jagielo, …, D. A. Schwartz. 1997. The kinetics of grain dust-induced inflammation of the lower respiratory tract. *Am. J. Respir. Crit. Care Med.* 155:254–259.
11. George, C. L. S., H. Jin, …, D. A. Schwartz. 2001. Endotoxin responsiveness and subchronic grain dust-induced airway disease. *Am. J. Physiol. Lung Cell. Mol. Physiol.* 280:L203–L213.
12. Brogden, K. A., R. C. Cutlip, and H. D. Lehmkuhl. 1986. Complexing of bacterial lipopolysaccharide with lung surfactant. *Infect. Immun.* 52:644–649.
13. Griese, M. 1999. Pulmonary surfactant in health and human lung diseases: state of the art. *Eur. Respir. J.* 13:1455–1476.
14. Sáenz, A., O. Cañadas, …, C. Casals. 2007. Effect of surfactant protein A on the physical properties and surface activity of KL4-surfactant. *Biophys. J.* 92:482–492.
15. Ruano, M. L., K. Nag, …, K. M. Keough. 1998. Differential partitioning of pulmonary surfactant protein SP-A into regions of monolayers of dipalmitoylphosphatidylcholine and dipalmitoylphosphatidylcholine/dipalmitoylphosphatidylglycerol. *Biophys. J.* 74:1101–1109.
16. Worthman, L. A., K. Nag, …, K. M. Keough. 2000. Pulmonary surfactant protein A interacts with gel-like regions in monolayers of pulmonary surfactant lipid extract. *Biophys. J.* 79:2657–2666.
17. Sánchez-Barbero, F., J. Strassner, …, C. Casals. 2005. Role of the degree of oligomerization in the structure and function of human surfactant protein A. *J. Biol. Chem.* 280:7659–7670.
18. Sánchez-Barbero, F., G. Rivas, …, C. Casals. 2007. Structural and functional differences among human surfactant proteins SP-A1, SP-A2 and co-expressed SP-A1/SP-A2: role of supratrimeric oligomerization. *Biochem. J.* 406:479–489.
19. Maget-Dana, R. 1999. The monolayer technique: a potent tool for studying the interfacial properties of antimicrobial and membrane-lytic peptides and their interactions with lipid membranes. *Biochim. Biophys. Acta.* 1462:109–140.
20. Smith, R. D., and J. C. Berg. 1980. The collapse of surfactant monolayers at the air-water interface. *J. Colloid Interface Sci.* 74:273–286.
21. Hac-Wydro, K., and P. Dynarowicz-Łatka. 2006. Nystatin in Langmuir monolayers at the air/water interface. *Colloids Surf. B Biointerfaces.* 53:64–71.
22. Nikaido, H. 2003. Molecular basis of bacterial outer membrane permeability revisited. *Microbiol. Mol. Biol. Rev.* 67:593–656.
23. Stamme, C., E. Walsh, and J. R. Wright. 2000. Surfactant protein A differentially regulates IFN-γ- and LPS-induced nitrite production by rat alveolar macrophages. *Am. J. Respir. Cell Mol. Biol.* 23:772–779.
24. Bufler, P., B. Schmidt, …, M. Griese. 2003. Surfactant protein A and D differently regulate the immune response to nonmucoid *Pseudomonas aeruginosa* and its lipopolysaccharide. *Am. J. Respir. Cell Mol. Biol.* 28:249–256.